

INTERACTION OF A MAIN CRACK WITH ORDERED DISTRIBUTIONS OF MICROCRACKS

A. Brencich and A. Carpinteri
Department of Structural Engineering, Politecnico di Torino,
Torino, Italy.

Abstract

The question whether the interaction of a main crack with distributions of microcracks is a short range phenomenon rises from some experimental evidences showing that a widely microcracked area develops in front of the main crack tip.

In the present work the phenomenon is investigated by means of a boundary element technique which proved to be reliable for weakly as well as for strongly interacting cracks. The interactions among microcracks are also taken into account. The results show that the amplification effects present a rather wider range than what is usually expected.

1 Introduction

The interaction of a main crack with a distribution of microcracks is usually considered a short range phenomenon as a result of the hypothesis of non interacting microcracks -dilute limit- which is usually

considered acceptable. The problem has thus been studied considering distributions of few microcracks, seldom more than three, or, at the most, periodic distributions of microcracks, and taking into account the interaction with the main crack by means of analytical methods, such as a point source representation of the microcracks (Rose, 1986), the complex potentials (Rubinstein, 1985) and the edge dislocation method (Lam et al., 1993), or numerical methods, such as the "method of pseudo-tractions" (Horii and Nemat-Nasser, 1985; Kachanov, 1987) resulting from a superposition scheme.

Experimental evidences (Han and Suresh, 1989; Hutchinson, 1987; Ruhle et al., 1987) show, on the contrary, that in brittle materials a wide microcracked process zone develops in front and around the main crack tip up to rather long distances, rising the question whether and to which extent the far located microcracks have any influence on the main crack.

The main difficulty is found in the development of analytical or numerical tools to consider generical geometries involving a multitude of microcracks without any periodical distribution.

In the present work the interaction of a main crack with different distributions of microcracks is taken into account through a boundary element technique based on displacement discontinuity elements. Such a technique has been found reliable with high precision, less than 1%, for strongly interacting as well as for weakly interacting microcracks. For shielding effects the phenomenon can be actually considered as short ranged, whereas for amplification effects the range is somewhat wider. These results are obtained taking into account the interaction of each microcrack with any other microcrack as well as with the main crack.

2 The numerical procedure

Let us consider an infinite plate of a linear elastic and isotropic material, and impose constant displacement jumps in the normal n and shear s directions along the segment $|\bar{x}| \leq a$, $\bar{y} = 0$ (fig. 1).

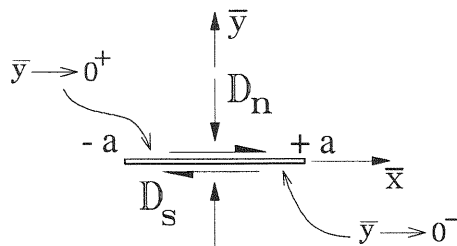


Fig. 1. Displacement discontinuities

Consider then a series of m segments like the one depicted in fig. 1. Taking into account the mutual and linear influence of any displacement discontinuity over each segment and summing up all the contributions, for each segment we can write (Crouch and Starfield, 1983):

$$u_n^i = \sum_{j=1}^m E_{nn}^{ij} D_n^j + \sum_{j=1}^m E_{ns}^{ij} D_s^j, \quad u_s^i = \sum_{j=1}^m E_{sn}^{ij} D_n^j + \sum_{j=1}^m E_{ss}^{ij} D_s^j, \quad (1.a,b)$$

$$\sigma_n^i = \sum_{j=1}^m F_{nn}^{ij} D_n^j + \sum_{j=1}^m F_{ns}^{ij} D_s^j, \quad \tau_s^i = \sum_{j=1}^m F_{sn}^{ij} D_n^j + \sum_{j=1}^m F_{ss}^{ij} D_s^j. \quad (2.a,b)$$

Any structural problem can thus be described by congruence and equilibrium equations like (1) and (2), which constitute a system of linear algebraic equations with the index i varying over the range $[1, m]$ for all the segments. The terms on the left-hand side of eqs. (1) and (2) represent the resulting effect, displacement or stress, due to all displacement discontinuities applied, thus representing the boundary conditions given over each segment. The system of equations describing the whole elastic problem can be obtained choosing the suitable relations from (1) and (2) according to the boundary conditions imposed.

Imagine to divide a crack into a series of m straight segments over which a constant displacement discontinuity is imposed in order to model the effective profile of the crack faces. The global problem can thus be divided into m subproblems, each consisting of a displacement discontinuity imposed to one segment on the crack line while no displacement discontinuity is imposed on the other segments (fig. 2).

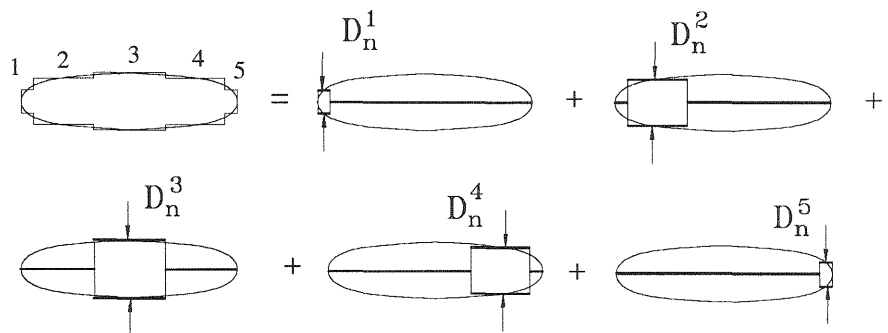


Fig. 2. Discretization of a crack with $m=5$ d. d. segments

Except for pressurised cracks, the boundary conditions related to the crack segments to impose on the left-hand side of the solving system are that the crack faces are stress free.

Once the displacement discontinuities are known, the SIFs can be directly evaluated through the following expressions (Carpinteri, 1986):

$$K_I = D_n(r) \frac{E}{4} \sqrt{\frac{\pi}{2r}}, \quad K_{II} = D_s(r) \frac{E}{4} \sqrt{\frac{\pi}{2r}}, \quad (3.a,b)$$

where $D_n(r)$ and $D_s(r)$ are the displacement discontinuities at a distance r from the crack tip, and E is the Young's modulus of the material.

3 Interaction of the main crack with ordered distributions of microcracks

Three different microcrack distributions have been considered (fig. 3): (a) eight microcracks, (b) eighteen microcracks, disposed on three columns and six rows; (c) fifty-six microcracks distributed on seven columns and eight rows.

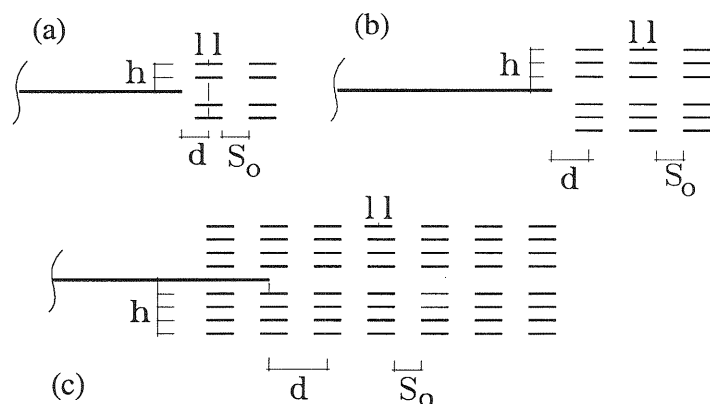


Fig. 3. Three kinds of geometric distributions of microcracks

The geometric parameters needed to describe each case, normalised by the microcrack half-length, are the vertical, h , and horizontal, S_o , spacings between microcracks, and the frontal distance d of a reference column from the main crack tip.

Varying the two spacings, more dense or more dispersed distributions of microcracks are obtained, from which stronger or weaker interactions are to be expected. As the parameter d changes, different values of the SIF at the main crack tip are obtained, amplified or shielded according to the parameter itself.

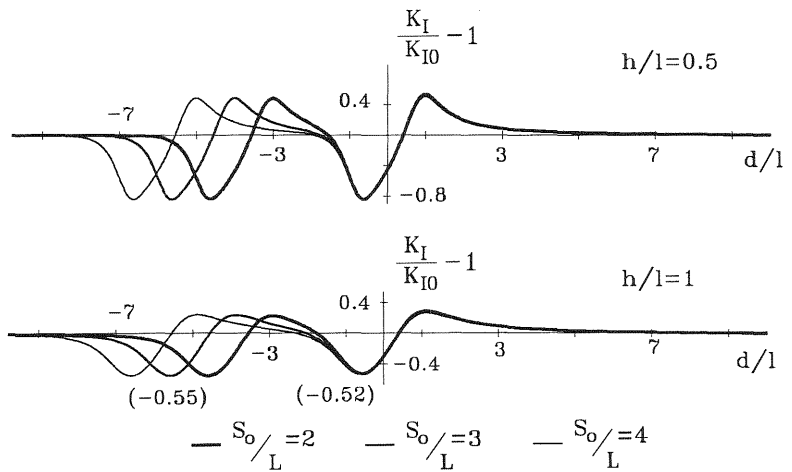


Fig. 4. Diagrams for the 8 microcrack geometry, $h/l=0.5$, $h/l=1.0$

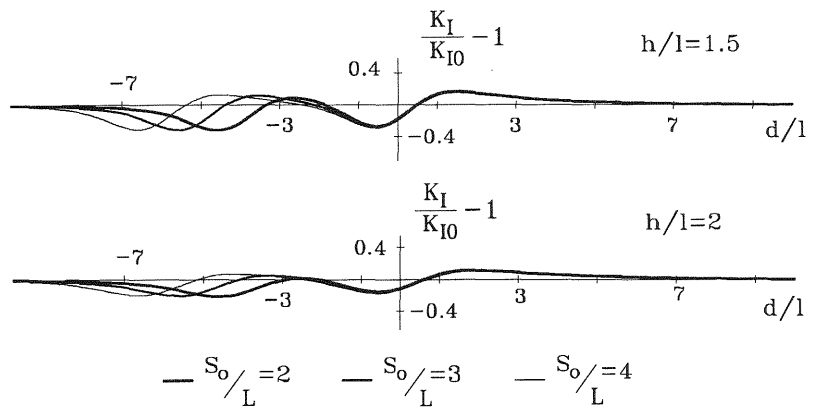


Fig. 5. Diagrams for the 8 microcrack geometry, $h/l=1.5$, $h/l=2.0$

Figures 4 and 5 present the twelve diagrams for the geometry with eight microcracks, while figures 6 and 7 present the same series for the 18 microcrack geometry.

Figure 8 refers to the 56 microcrack geometry in the case $S_0/l=2$ (analogous diagrams can be obtained for different horizontal spacings).

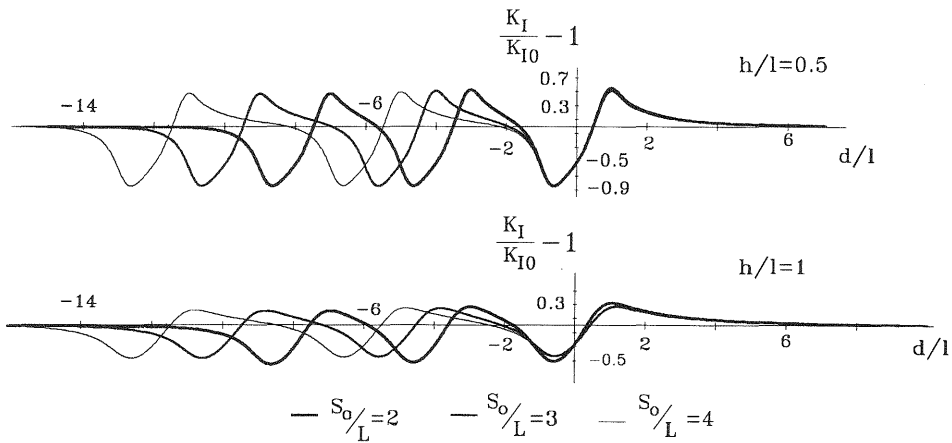


Fig. 6. Diagrams for the 18 microcrack geometry, $h/l=0.5$, $h/l=1.0$

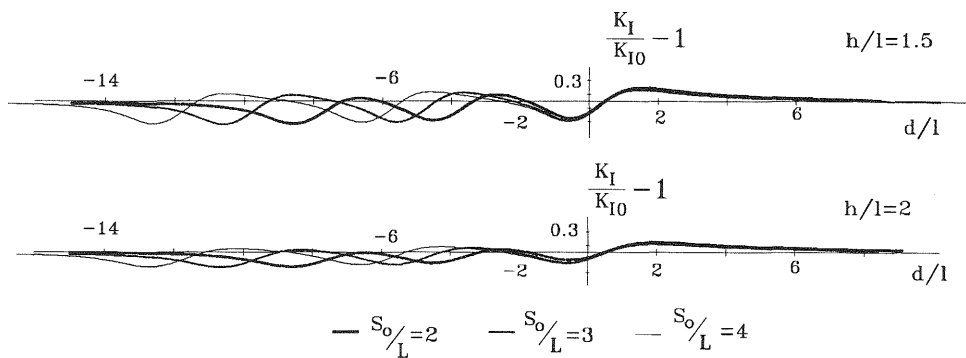


Fig. 7. Diagrams for the 18 microcrack geometry, $h/l=1.5$, $h/l=2.0$

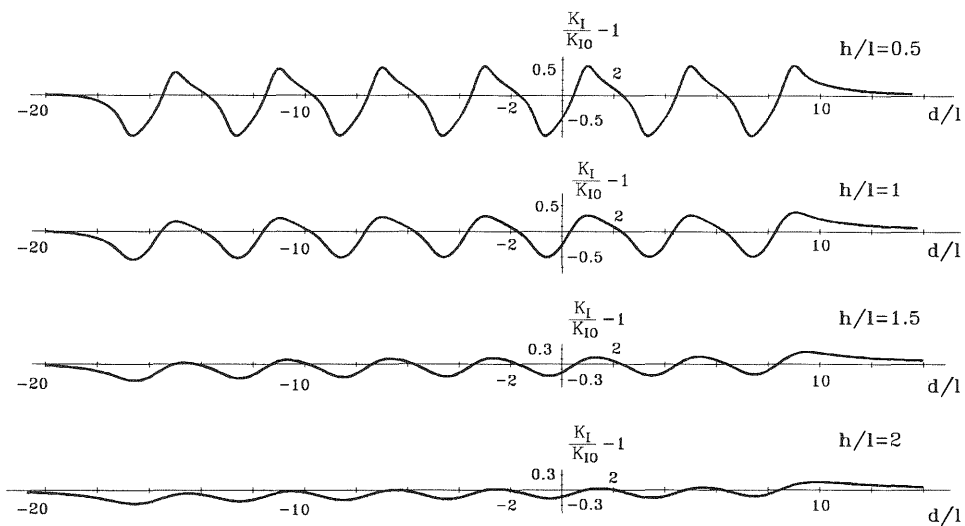


Fig. 8. Fiftysix microcrack array, $S_0/l=2$

4 Discussion on the numerical results

The comparison of the diagrams with the same vertical spacing h / l shows that the horizontal spacing has a small influence on the phenomenon.

The diagrams present a number of relative minima and maxima coincident with the number of columns, corresponding each maximum (minimum) to the position of the microcrack array in which a single column presents a prevailing role in the amplification (shielding) phenomenon. The absolute variation of these peak values is hardly significant. Changing the vertical spacing h is of much greater effect. As the parameter h / l increases, both the amplification and shielding effects rapidly decrease. The diagrams remain asymmetric and the peak values are so sharply cut down that a vertical distance h equal to 2.5 times the microcrack half-length can be considered the limit for negligible interactions.

Each geometry presents a "neutral position", identified by values of the front distance d / l in the range [0.3,0.8], for which the SIF at the main crack tip is the same as that for the undamaged material. Computing the angle between an horizontal line and a segment joining the main crack tip and the centre of the closest microcrack (fig. 9) the values of Table 1 are obtained ($S_o/l = 3$).

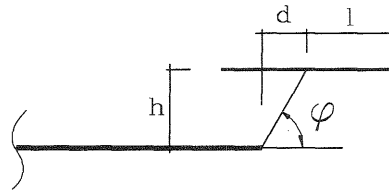


Fig. 9. Angle between the horizontal line and a microcrack centre

Table 1. Angles corresponding to the neutral positions ($S_o/l = 3$)

h / l	2 microcracks	8 microcracks	18 microcracks	56 microcracks
0.5	$\varphi = 47^\circ$	$\varphi = 51^\circ$	$\varphi = 47^\circ$	$\varphi = 50^\circ$
1.0	$\varphi = 63^\circ$	$\varphi = 69^\circ$	$\varphi = 71^\circ$	$\varphi = 72^\circ$
1.5	$\varphi = 68^\circ$	$\varphi = 72^\circ$	$\varphi = 74^\circ$	$\varphi = 71^\circ$
2.0	$\varphi = 68^\circ$	$\varphi = 73^\circ$	$\varphi = 75^\circ$	$\varphi = 70^\circ$

While angle φ is about seventy degrees for the three geometries with $h/l = 1.0, 1.5$ and 2.0 , it is interesting to point out that strong interactions ($h/l = 0.5$) lowers this angle to about fifty degrees.

Analogous considerations can be made for the position of relative maximum obtainable for values of the parameter d/l in the range $[1,2]$.

Table 2 summarizes the angles, as defined in figure 9, for which the maximum amplification is found.

Table 2. Angles corresponding to the maximum amplification ($S_o/l = 3$)

h/l	2 microcracks	8 microcracks	18 microcracks	56 microcracks
0.5	$\varphi = 27^\circ$	$\varphi = 27^\circ$	$\varphi = 27^\circ$	$\varphi = 27^\circ$
1.0	$\varphi = 41^\circ$	$\varphi = 45^\circ$	$\varphi = 42^\circ$	$\varphi = 45^\circ$
1.5	$\varphi = 45^\circ$	$\varphi = 47^\circ$	$\varphi = 45^\circ$	$\varphi = 49^\circ$
2.0	$\varphi = 47^\circ$	$\varphi = 48^\circ$	$\varphi = 45^\circ$	$\varphi = 47^\circ$

Table 3. Angles corresponding to the maximum shielding ($S_o/l = 3$)

h/l	0.5	1.0	1.5	2.0
φ	140°	121°	112°	107°

On the contrary, the maximum shielding position is obtained always for a frontal distance d/l equal to -0.6 , corresponding, case by case, to the angles reported in Table 3. Amplification and shielding cannot be considered as symmetrical phenomena.

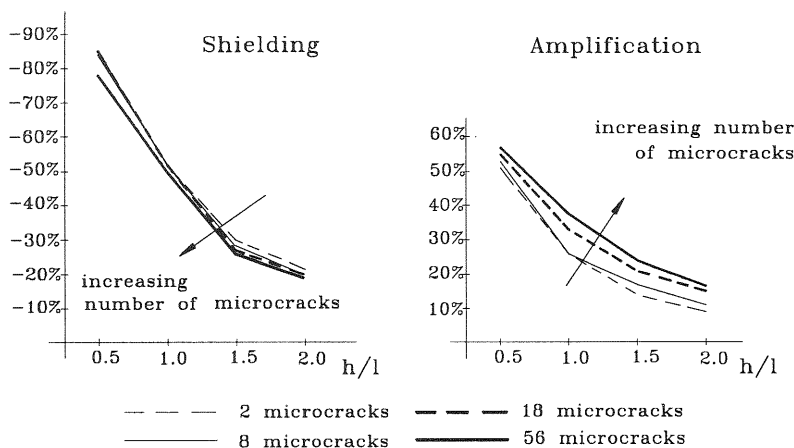


Fig. 10. Maximum amplification and shielding as function of the vertical spacing and microcrack number ($S_o/l = 2$)

The diagrams in figure 10 are obtained considering the absolute maximum and minimum values of the SIF at the main crack tip.

It can be seen that the maximum shielding is almost unaffected by the number of microcracks, and can be considered a short-range effect. The maximum amplification, on the other hand, is significantly altered by the number of microcracks as much that, for $h/l = 2.0$, the amplification due to fifty-six microcracks is almost twice that due to two microcracks.

5 Conclusions

The macrocrack-microcrack interaction is usually considered a short range phenomenon involving only few of the closest microcracks. This was found true, to some extent, only for shielding of the main crack which seems to be almost unaffected by the number of microcracks (figure 10). On the contrary, the amplification of the SIF at the main crack tip is significantly altered by far located microcracks. Thus the amplification range has to be considered wider than the shielding range, as was confirmed also by other authors through a double layer potential technique (Dolgopolsky et al., 1989).

In some materials, like ceramics, damage is modelled by means of random microcrack distributions (Haung and Karihaloo, 1993; Laures and Kachanov, 1991; Brencich et al.) located in front of the main crack. Experimental investigations (Han and Suresh, 1989) show that this process zone is quite long in front of the main crack tip. The results presented in this paper go further in this direction, giving some reasons for taking into account distant microcracks, the interaction of which has been found not negligible *a priori*.

6 Acknowledgements

The authors gratefully acknowledge the financial support of the National Research Council (CNR) and the Department for University and Scientific and Technological Research (MURST).

7 References

- Brencich A., Carpinteri A., Scavia C., Disorder effects on the interaction between a main crack and a distribution of microcracks, submitted for publication in the **J. of Applied Mechanics** (ASME).
- Carpinteri A. (1986) **Mechanical Damage and Crack Growth in Concrete**, Martinus Nijhoff, Dordrecht.
- Crouch S.L, Starfield A.M. (1983) **Boundary Element Methods in Solid Mechanics**, Unwin Hyman, Cambridge.
- Dolgopolsky A., Karbhari V., Kwak S.S. (1989) Microcrack induced toughening - an interaction model, **Acta Metall.**, 37, 1349-1354.
- Han L.X., Suresh S. (1989) High-temperature failure of an Alumina-Silicon Carbide composite under cyclic loads: mechanisms of fatigue crack tip damage, **J. Am. Ceram. Soc.**, 72, 1233-1238.
- Horii H., Nemat-Nasser S. (1985) Elastic fields of interacting inhomogeneities, **Int. J. Sol. Str.**, 21, 731-745.
- Huang X., Karihaloo B.L. (1993) Interaction of penny shaped cracks with a half plane crack, **Int. J. Sol. Str.**, 25, 591-607.
- Hutchinson J.W. (1987) Crack tip shielding by micro-cracking in brittle solids, **Acta Metall.**, 35 , 1609-1619.
- Kachanov M. (1987) Elastic solids with many cracks: a simple method of analysis, **Int. J. Sol. Str.**, 23, 23-43.
- Lam K.Y., Wen C., Phua Z. (1993) Interaction between microcracks and a main crack in a semi-infinite medium, **Eng. Fr. Mech.**, 44, 753-761.
- Laures J.P., Kachanov M. (1991) Three dimensional interactions of a crack front with arrays of penny-shaped microcracks, **Int. J. Fract.**, 48, 255-279.
- Rose L.R. (1986) Microcrack interaction with a main crack, **Int. J. Fract.**, 31, 233-242.
- Rubinstein A.A. (1985) Macrocrack interaction with semi-infinite microcrack array, **Int. J. Fract.**, 27, 113-119.
- Ruhle M., Evans A.G., McMeeking R.M. (1987) Charalambides P.G., Hutchinson J.W., Microcrack toughening in Alumina/Zirconia, **Acta Metall.**, 35 , 2701-2710.